

## Article

# Comparing the Urban Floods Resistance of Common Tree Species in Winter City Parks

Chang Zhai <sup>1</sup>, Zhonghui Zhang <sup>2,\*</sup>, Guangdao Bao <sup>2,\*</sup>, Dan Zhang <sup>1</sup>, Ting Liu <sup>2</sup>, Jiaqi Chen <sup>1</sup>, Mingming Ding <sup>1</sup>, Ruoxuan Geng <sup>1</sup> and Ning Fang <sup>1</sup>

<sup>1</sup> College of Landscape Architecture, Changchun University, Changchun 130022, China

<sup>2</sup> Institute of Forest Management, Jilin Provincial Academy of Forestry Sciences, Changchun 130033, China

\* Correspondence: zzhgiszzh@163.com (Z.Z.); bao-gd@126.com (G.B.)

**Abstract:** The rapid urbanization process and high-intensity construction mode have greatly changed the underlying surface structure and spatial distribution of the natural land surface, further amplified the possibility of urban floods, and made urban security face more serious threats. Urban forest could help to mitigate urban floods through water holding and interception by its unique structures, especially the litter layer. This paper compared the ability of different forest tree species on urban floods mitigation, through analyzing their litter accumulation, litter water holding characteristics, and water interception features of different decomposed layers. The results concluded that *Quercus mongolica* Fisch. ex Ledeb. (QM) forest, *Betula platyphylla* Sukaczew (BP) forest, *Larix gmelinii* (Rupr.) Kuzen. (LG) forest, and *Picea koraiensis* Nakai (PK) forest were the best choices for improving urban floods resistance in a high-urbanization winter city, for they had larger litter mass and higher maximum water holding and interception capacity. The corresponding results of this study could help environmental management departments worldwide in the selection of tree species in urban greening projects focusing on urban flood control.



**Citation:** Zhai, C.; Zhang, Z.; Bao, G.; Zhang, D.; Liu, T.; Chen, J.; Ding, M.; Geng, R.; Fang, N. Comparing the Urban Floods Resistance of Common Tree Species in Winter City Parks. *Land* **2022**, *11*, 2247. <https://doi.org/10.3390/land11122247>

Academic Editors: Zhifang Wang, Salman Qureshi, Guangsi Lin, Mohammed Almahood and Wenwen Cheng

Received: 11 November 2022

Accepted: 8 December 2022

Published: 9 December 2022

**Publisher's Note:** MDPI stays neutral with regard to jurisdictional claims in published maps and institutional affiliations.



**Copyright:** © 2022 by the authors. Licensee MDPI, Basel, Switzerland. This article is an open access article distributed under the terms and conditions of the Creative Commons Attribution (CC BY) license (<https://creativecommons.org/licenses/by/4.0/>).

**Keywords:** hydrological characteristics; litter accumulation; urban floods; urban forest

## 1. Introduction

The Intergovernmental Panel on Climate Change (IPCC) sixth assessment report (AR6) stated that human-induced climate change, including more frequent and intense extreme events, has caused widespread adverse impacts and related losses and damages to nature and people [1]. Among this, heavy precipitation events were one of the climate and weather extremes that had widespread, pervasive impacts on ecosystems, people, settlements, and infrastructure [2,3]. For example, extreme rainfall, which was enhanced by the moisture influx ahead of Typhoon In-fa, hit Henan province in central China from 17 to 21 July 2021. The most severely affected area was around the city of Zhengzhou (the capital of Henan Province), which, on 20 July, received 201.9 mm of rainfall in one hour (a Chinese national record) and 382 mm in 6 h. For the event as a whole, the area received 720 mm, more than its annual average. The city experienced extreme flash flooding, with many buildings, roads, and subways inundated. The flooding was associated with 380 deaths or missing persons, and economic losses of USD 17.7 billion were reported [1,4]. Moreover, from mid to late July to August 2021, Jincheng city in Shanxi Province, Suizhou city in Hubei Province, and Lantian city in Shaanxi Province experienced extremely heavy rainfall, causing serious urban flooding. The direct economic loss in China was USD 35.13 billion in 2021 [5]. Consequently, strengthening the ability to prevent urban flood disasters has become an important issue of sustainable urban development and the UN's 2030 Sustainable Development Goals (SDGs) under the topic of sustainable cities and human settlements [6].

Frequent urban floods have brought more and more negative effects on urban infrastructure and economy [7–10]. It is a natural phenomenon in which heavy rain falls on the

complex underlying surface of the city and the runoff cannot be discharged in time, thus causing surface water accumulation [11–13]. Urbanization-induced construction changes its micro-topography, which may hinder urban flood management [7]. Specifically, the manmade land covers destroy the original urban hydrological cycle, which impedes the natural infiltration of rainwater and reduces the storage capacity of the underlying urban surface [8]. Previous studies concluded that urban floods are caused by both natural and human factors [14,15]. In terms of natural factors, extreme precipitation events caused by climate change significantly increase the probability of floods [8,12,16]. More importantly, in recent years, the precipitation in many cities has been significantly higher than that in surrounding suburbs, forming the “urban rain island” effect, which has made urban flooding events occur more frequently [8]. In addition to uncontrollable natural factors, unreasonable territorial space planning is also an important cause of urban floods [17]. The rapid increase in urban impervious surfaces has made it difficult for surface runoff to penetrate and has weakened the rainwater regulation ability of the ecosystem [18]. It was proved that there is a significant correlation between impervious surface density and flood probability [19]. The formation from rainfall to flood is a nonlinear complex physical process, which is affected by multiple factors [20–22], among which the spatial pattern of the urban underlying surface is one of the important influencing factors [19,23].

Some concepts aiming to mitigate urban floods have been put forward in many countries, for instance, the “Best Management Practice” from the United States, the “Sustainable Drainage System” of the United Kingdom, the “Low Impact Development” from New Zealand, the “Water Sensitive City” from Australia [24–27], and the “Sponge City” of China [28–30], while the application of green infrastructure is the main part for implementing such concepts [20,22,31]. Urban forest is the ecological infrastructure that the urban system depends on and plays important roles in the urban hydrological cycle [32,33]. On the one hand, the forest ecosystem realizes the redistribution and effective regulation of atmospheric precipitation through its lush canopy [32,34,35]; on the other hand, the developed shrub layer, the dense forest litter layer, and the loose and deep soil layer in the forest ecosystem play a role in regulating and storing the water process, creating a superior environment for the interception and storage of precipitation, and playing the unique water conservation function [36,37]. However, the forest canopy and trunk will reach saturation under a high intensity or large amount of rainfall. In this case, the litters play the main part in its powerful function of rainwater regulation and storage. However, the litters are usually cleaned up and disposed as garbage under the cities’ environmental cleanliness requirements, especially for the litters along the roads and in the communities [38]. Nevertheless, the mitigation of urban flood resistance ability can be released by litters in urban parks [39]. The forests existing in urban parks are managed well, and the litters can be a strong weapon to defend against urban flooding events. Under such circumstances, a comparison or ranking of different tree species on litters’ water retention ability at different rainfall scenarios is essential for the future construction of water conservation forest in urban land.

In this paper, Changchun city, which is a typical winter city undergoing rapid urbanization, was selected as the study area. Winter cities are a special urban group in the Northern Hemisphere characterized by long harsh winters (i.e., mean January temperatures below  $-18\text{ }^{\circ}\text{C}$ ) and usually unique forest landscapes [40,41]. We analyzed the litter accumulative amount, water holding, and interception characteristics of 14 tree species, and revealed their suitability for selection as urban flood resistance, by means of field investigation, laboratory experiment, and statistical analysis. Moreover, our research attempted to provide some useful suggestions to assist environmental management departments in selecting proper tree species if they try to use urban trees as an urban-flood-resistant tool. The findings are also applicable to other cities with similar climate conditions that are suffering or will experience disasters caused by heavy rains. Specifically, the objectives of this study were: (1) to determine the litter accumulation difference among different tree

species; (2) to identify their water hydrological characteristics, and (3) to make a suggestion on tree species selection for urban flood mitigation.

## 2. Materials and Methods

### 2.1. Study Area

Changchun city (43°05′–45°15′ N; 124°18′–127°05′ E) is the capital of Jilin Province, located in the middle latitude of the Northern Hemisphere, the hinterland of the Northeastern Plain of China [42]. The built-up area is 543 km<sup>2</sup>, with a population of 4.468 million at the end of 2020. Changchun is located in the warm temperate zone, which is a continental monsoon climate area, with an annual average temperature of 7.1 °C, annual precipitation of 662 mm, and annual sunshine duration of 2688 h in 2020. The altitude is 250–350 m in Changchun, and the main types of soil are black soil, meadow soil, and chernozem soil. The vegetation area is 228.65 km<sup>2</sup> and the coverage rate is 42.11% [43]. With the intensification of global change and urbanization, Changchun is facing the possibility of a surge in the rise in rainfall, which could increase the probability of urban floods. The Statistical Yearbook of Jilin Province indicated that the rainfall of Changchun reached 273.2 mm in September 2020 [42], which is six times the mean value from 2016 to 2019 of the same month [44–47]. In this study, 14 sample plots were set in Nanhu Park, Changchun Park, and Hundred Trees Park. The basic information of the plots is shown in Table 1.

**Table 1.** Basic condition of 14 forest stand types. Note: Tree height and breast diameter are shown as mean ± SD.

Forest Stands	Abbr.	Canopy Density	Average Tree Height (m)	Mean Breast Diameter (cm)	Plot Coordinates	Forest Density (Trees/Plot)
<i>Quercus mongolica</i> Fisch. ex Ledeb. forest	QM forest	0.85	9.92 ± 1.2	16.5 ± 2.6	43°51′04″ N 125°17′39″ E	40
<i>Betula platyphylla</i> Sukaczew forest	BP forest	0.89	18.04 ± 3.1	24.9 ± 2.8	43°50′57″ N 125°18′12″ E	36
<i>Salix matsudana</i> Koidz. forest	SM forest	0.81	7.80 ± 1.7	17.6 ± 2.2	43°53′45″ N 125°16′13″ E	20
<i>Armeniaca sibirica</i> (L.) Lam. Forest	AS forest	0.77	5.80 ± 1.1	16.3 ± 3.8	43°53′15″ N 125°16′13″ E	19
<i>Padus virginiana</i> ‘Canada Red’ forest	PV forest	0.75	3.70 ± 0.2	5.0 ± 0.6	43°52′34″ N 125°21′14″ E	27
<i>Populus alba</i> × <i>P. Berolinensis</i> forest	PA forest	0.77	12.80 ± 0.5	17.9 ± 2.3	43°52′28″ N 125°21′19″ E	22
<i>Tilia amurensis</i> Rupr. forest	TA forest	0.81	6.90 ± 1.3	21.8 ± 1.9	43°53′17″ N 125°16′10″ E	16
<i>Ginkgo biloba</i> L. forest	GB forest	0.72	6.30 ± 0.2	17.3 ± 4.8	43°53′45″ N 125°16′13″ E	19
<i>Amygdalus persica</i> f. rubro-plena forest	AP forest	0.78	6.50 ± 0.3	10.9 ± 1.1	43°53′36″ N 125°16′14″ E	27
<i>Pinus sylvestris</i> L. var. <i>mongolica</i> Litv. forest	PS forest	0.93	10.64 ± 1.4	20.2 ± 4.6	43°51′04″ N 125°17′40″ E	39
<i>Larix gmelinii</i> (Rupr.) Kuzen. forest	LG forest	0.78	13.57 ± 2.1	24.9 ± 6.3	43°50′58″ N 125°17′13″ E	21
<i>Pinus tabulaeformis</i> var. <i>mukdensis</i> forest	PT forest	0.73	11.80 ± 1.0	31.0 ± 5.8	43°51′17″ N 125°17′57″ E	6
<i>Abies holophylla</i> Maxim. forest	AH forest	0.82	15.70 ± 1.9	23.1 ± 6.5	43°50′57″ N 125°17′09″ E	15
<i>Picea koraiensis</i> Nakai forest	PK forest	0.85	14.30 ± 1.8	23.4 ± 2.8	43°50′57″ N 125°17′09″ E	17

## 2.2. Methods

### 2.2.1. Litter Collection and Accumulation Calculation

Sample plots over 20 m × 20 m were set-up for each forest stand in November 2021. In each plot, we selected three 1 m × 1 m quadrats randomly in the diagonal direction, and all litters in the quadrat were collected into plastic bags and weighed immediately according to the un-decomposed layer and semi-decomposed layer [48]. The litters of different layers were weighed after indoor air drying, and then the dry weight per unit area of the two layers was calculated [48,49].

### 2.2.2. Measure the Hydrological Characteristics of Different Forest Stands

The water holding process of litter was determined by the indoor immersion method [49]. After the litters were air-dried, they were placed into a mesh bag with a hole diameter of 1 mm and immersed in water, and it was ensured that the litters were submerged under the water surface. After absorbing water for 5 min, 10 min, 15 min, 30 min, 1 h, 2 h, 4 h, 6 h, 8 h, 10 h, 12 h, and 24 h, it was taken out and suspended for a few minutes. When the bag with litter was no longer dripping, it was weighed to calculate the water holding rate and water holding capacity at each moment. The litter soaked in water for 24 h was placed in the ventilation place to air-dry. Each sample was repeated three times. The methodology of this study is shown in Figure 1.

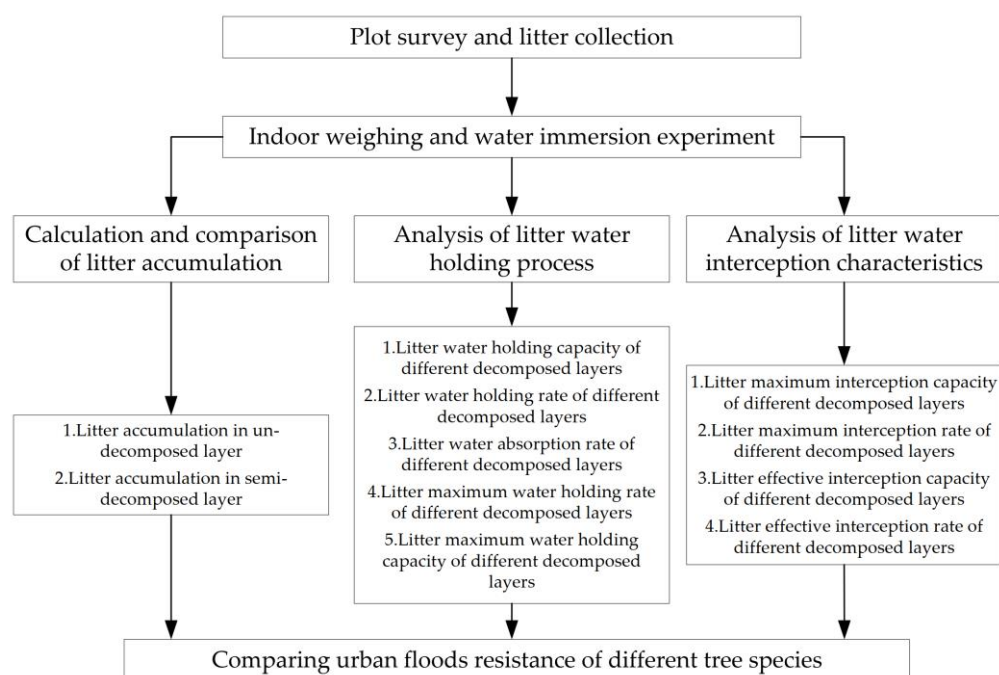


**Figure 1.** Flow chart of the methodology.

The water holding rate, water holding capacity, water absorption rate, maximum water holding rate, maximum water holding capacity, maximum water interception rate, maximum water interception capacity, effective interception rate, and effective interception capacity of litter were calculated according to the formulas [36,49] in Table 2.

**Table 2.** The hydrological parameters of litters.

Hydrological Parameters of Litters	Abbr.	Units	Equations	Explanations
Water holding capacity	$W_t$	$\text{kg}/\text{m}^2$	$W_t = G_t - G_d$	$G_t$ is the wet weight of litter at time $t$ ( $\text{kg}/\text{m}^2$ ); $G_d$ is the dry weight of litter ( $\text{kg}/\text{m}^2$ ).
Water holding rate	$R_h$	%	$R_h = (G_t - G_d)/G_d \times 100\%$	Same as above.
Water absorption rate in a certain period	$V$	$\text{kg}/\text{m}^2/\text{h}$	$V = W_t/t$	$W_t$ is water holding capacity at time $t$ .
Maximum water holding rate	$R_{h \max}$	%	$R_{h \max} = (G_{24} - G_d)/G_d \times 100\%$	$G_{24}$ is the weight of litter soaked in water for 24 h ( $\text{kg}/\text{m}^2$ ); $G_d$ is the dry weight of litter ( $\text{kg}/\text{m}^2$ ).
Maximum water holding capacity	$W_{h \max}$	$\text{kg}/\text{m}^2$	$W_{h \max} = M \times R_{h \max}$	$R_{h \max}$ is the maximum water holding rate (%); $M$ is litter accumulation ( $\text{kg}/\text{m}^2$ ).
Average natural water content	$R_0$	%	$R_0 = (G_0 - G_d)/G_d \times 100\%$	$G_0$ is the fresh weight of litter ( $\text{kg}/\text{m}^2$ ); $G_d$ is the dry weight of litter ( $\text{kg}/\text{m}^2$ ).
Maximum interception rate	$R_{s \max}$	%	$R_{s \max} = R_{h \max} - R_0$	$R_{h \max}$ is the maximum water holding rate (%); $R_0$ is the average natural water content (%).
Maximum interception capacity	$W_{s \max}$	$\text{kg}/\text{m}^2$	$W_{s \max} = R_{s \max} \times M$	$R_{s \max}$ is the maximum litter interception rate (%); $M$ is litter accumulation ( $\text{kg}/\text{m}^2$ ).
Effective interception rate	$R_{sv}$	%	$R_{sv} = 0.85R_{h \max} - R_0$	$R_{h \max}$ is the maximum water holding rate (%); $R_0$ is the average natural water content (%).
Effective interception capacity	$W_{sv}$	$\text{kg}/\text{m}^2$	$W_{sv} = R_{sv} \times M$	$R_{sv}$ is the effective interception rate (%); $M$ is litter accumulation ( $\text{kg}/\text{m}^2$ ).

### 2.2.3. Data Analysis

All statistical analyses were performed by R software 4.2.2 (<http://cran.r-project.org>, accessed on 15 October 2022). Litter accumulation, water holding capacity, and interception characteristics of different forest types and different decomposed layers were detected by one-way ANOVA conducted with the function “aov”, and the Duncan test from package “agricolae” [50] was used for multiple comparisons with a significance level of 0.05. The figures were drawn by package “ggplot2” [51].

## 3. Results

### 3.1. Litter Accumulation and Composition of Different Forest Stands

The total accumulative amount of litter in each stand ranged from 0.24 to 1.99  $\text{kg}/\text{m}^2$  (Table 3). Except for QM forest, the total accumulation of coniferous forest stands was significantly higher than that of broadleaved forest stands ( $p < 0.05$ ), and the total accumulation of QM forest was also significantly higher than that of the other eight broadleaved forests ( $p < 0.05$ ). In the un-decomposed layer ( $p < 0.05$ ), the accumulative amount of PK forest was significantly larger than that of the other forest stands, and that of AH forest and QM forest were significantly higher than that of the other forest stands ( $p < 0.05$ ); moreover, the accumulation of AH forest in this layer accounted for 70.18% of its total. In the semi-decomposed layer, except BP forest and QM forest, the accumulation of coniferous forest stands was significantly higher than that of broadleaved forest stands ( $p < 0.05$ ); the highest value was LG forest, which reached 1.47  $\text{kg}/\text{m}^2$ , and the accumulative amount of the semi-decomposed layer accounted for 86.19% of the total value. PT forest had the second largest quantity, which was significantly larger than that of the other 12 species ( $p < 0.05$ ), while GB forest ranked last in the semi-decomposed layer, significantly smaller than that of QM forest, BP forest, PS forest, LG forest, PT forest, AH forest, and PK forest ( $p < 0.05$ ).

**Table 3.** Litter accumulation (mean  $\pm$  SD) in different decomposition degrees. Note: Different lowercase letters indicate significant differences among tree species at the 0.05 level. U indicates un-decomposed layer and S indicates semi-decomposed layer. The abbreviation of tree species is the same as Table 1.

Forest Stands	Total Accumulation (kg/m <sup>2</sup> )	U		S	
		Accumulation (kg/m <sup>2</sup> )	Proportions (%)	Accumulation (kg/m <sup>2</sup> )	Proportions (%)
QM forest	1.18 $\pm$ 0.0 d	0.70 $\pm$ 0.2 c	59.46	0.48 $\pm$ 0.1 de	40.54
BP forest	0.89 $\pm$ 0.1 e	0.24 $\pm$ 0.1 de	27.35	0.65 $\pm$ 0.1 cd	72.65
SM forest	0.34 $\pm$ 0.1 fg	0.14 $\pm$ 0.1 ef	39.94	0.20 $\pm$ 0.1 ef	60.06
AS forest	0.49 $\pm$ 0.1 f	0.29 $\pm$ 0.1 d	60.12	0.20 $\pm$ 0.1 ef	39.88
PV forest	0.50 $\pm$ 0.0 f	0.26 $\pm$ 0.1 de	51.49	0.24 $\pm$ 0.1 ef	48.51
PA forest	0.37 $\pm$ 0.0 fg	0.13 $\pm$ 0.0 ef	35.37	0.24 $\pm$ 0.1 ef	64.63
TA forest	0.24 $\pm$ 0.0 g	0.06 $\pm$ 0.0 f	24.79	0.18 $\pm$ 0.0 ef	75.21
GB forest	0.33 $\pm$ 0.1 fg	0.21 $\pm$ 0.0 def	64.02	0.12 $\pm$ 0.0 f	35.98
AP forest	0.36 $\pm$ 0.0 fg	0.13 $\pm$ 0.1 ef	37.47	0.23 $\pm$ 0.0 ef	62.53
PS forest	1.14 $\pm$ 0.2 d	0.29 $\pm$ 0.1 de	25.09	0.85 $\pm$ 0.3 c	74.91
LG forest	1.70 $\pm$ 0.1 b	0.23 $\pm$ 0.0 de	13.81	1.47 $\pm$ 0.0 a	86.19
PT forest	1.44 $\pm$ 0.0 c	0.26 $\pm$ 0.0 de	18.35	1.18 $\pm$ 0.0 b	81.65
AH forest	1.29 $\pm$ 0.1 cd	0.91 $\pm$ 0.1 b	70.18	0.38 $\pm$ 0.1 def	29.82
PK forest	1.99 $\pm$ 0.1 a	1.22 $\pm$ 0.1 a	61.32	0.77 $\pm$ 0.1 c	38.68

### 3.2. Litter Hydrological Characteristics

#### 3.2.1. Litter Water Holding Process

In general, the litter water holding capacity of each decomposition layer increased first and then tended to be stable with the increase in soaking time (Figure 2A–D). The results showed that the growth rate was relatively rapid in 0–2 h, stable in 2–12 h, and tended to be saturated in 12–24 h. In the un-decomposed layer, the 0–2 h water holding capacity in QM forest increased fastest, and the peak water holding capacity appeared earliest (Figure 2A). Moreover, the water holding capacity of PK forest ranked second after QM forest, but the values of PS forest, PT forest, PA forest, SM forest, and TA forest had little changes in 24 h. In addition, the peak values were not obvious, and the values were relatively low (Figure 2A,B). The variation trend of litters in the semi-decomposed layer was slightly moderate compared to that in the un-decomposed layer, and the increasing rate of litters in LG forest was largest. Except AH forest, the water holding capacity of coniferous forest stands was higher than that of broadleaved forest stands (Figure 2C,D).

The water holding rate in the two litter layers of different stand types was different (Figure 2E–H). Apparently, the five coniferous forest stands had a lower rate than the other nine broadleaved stands in the un-decomposed layer. GB forest, BP forest, and AP forest had a stronger water holding ability, especially for AP forest, which had a powerful ability to absorb water even after 8 h (Figure 2E,F). Moreover, almost all forest stands demonstrated a higher water holding rate in the semi-decomposed layer than the un-decomposed layer, except GB forest, which also had the lowest value before 1 h. However, GB forest as well as SM forest, AS forest, PV forest, PA forest, TA forest, and AP forest had a steady increasing trend from the beginning to 24 h (Figure 2G,H).

It can be concluded from Figure 2I–L that the changing trend of water absorption rate of two litter layers with soaking time was basically the same among different stand types. The water absorption rate of all stand types decreased linearly from 0 to 1 h of immersion, and then the decline rate gradually slowed down until 12 h, the curve tended to be consistent, and the water absorption of litters was close to saturation. QM forest, PK forest, and AH forest had a stronger water absorption ability than other stands in the un-decomposed layer. However, in the semi-decomposed layer, QM forest had a medium water absorption capacity. The five stand types with the highest water absorption capacity were LG forest, PT forest, PK forest, PS forest, and BP forest. Moreover, the 15 min water

absorption rate of LG forest could reach 399.31%, and the 0.5 h water absorption rate was up to 82.22%.

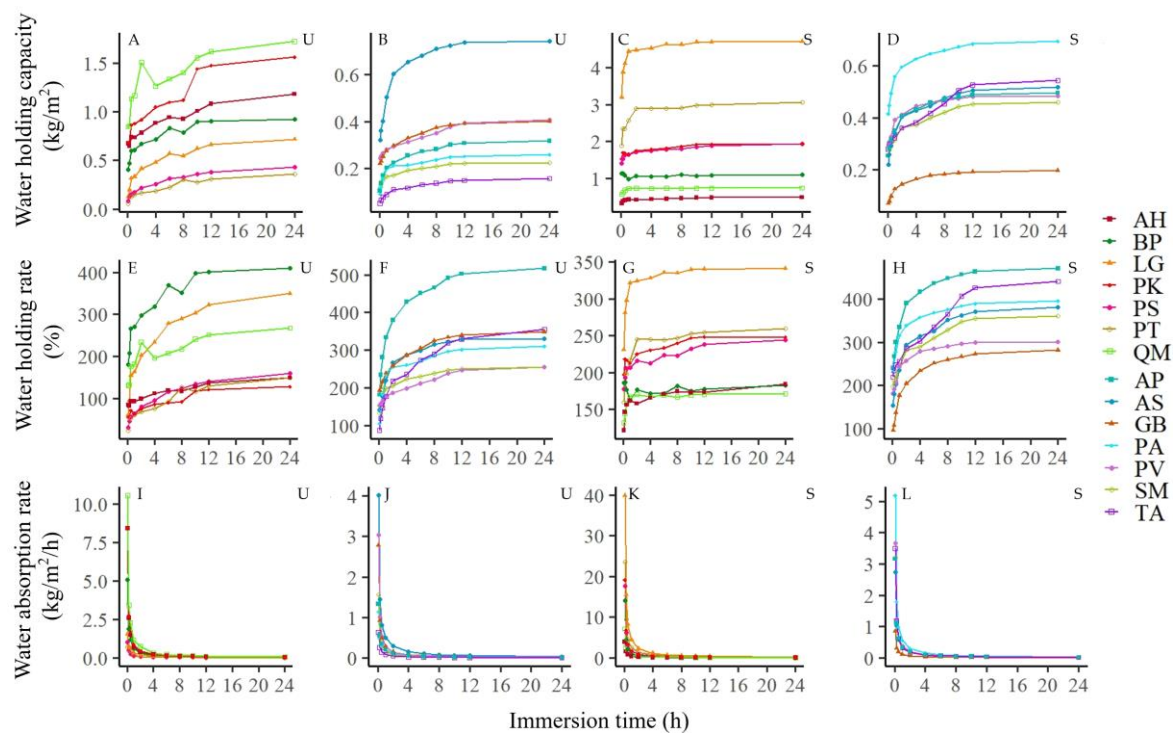


**Figure 2.** Relationship between litter water holding capacity (A–D), water holding rate (E–H), water absorption rate (I–L), and immersion time (h) of different tree species in different decomposed layers. Note: U indicates un-decomposed layer and S indicates semi-decomposed layer. Please see Table 1 for the abbreviation of tree species.

As shown in Table 4, the maximum water holding rate of the un-decomposed layer ranged from 135.50 to 517.05%, and the highest value was AP forest, which also had a significantly higher value than the other stands did ( $p < 0.05$ ), and 3.82 times the lowest value of PK forest. In addition, except for LG forest, the coniferous forest stands had significantly lower values than the eight broadleaved forests did ( $p < 0.05$ ). In the semi-decomposed layer, the maximum water holding rate was displayed as follows: AP forest > TA forest > PA forest > AS forest > SM forest > LG forest > PV forest > QM forest > GB forest > PS forest > PT forest > PK forest > BP forest > AH forest. AP forest had significantly larger values than QM forest, BP forest, SM forest, PV forest, GB forest, PS forest, and the other five coniferous species did ( $p < 0.05$ ). The maximum water holding capacity of QM forest was highest in the undecomposed layer, which was 7.58 times the lowest value (TA forest), and significantly higher (except PK forest) than those of the other 12 forest stands ( $p < 0.05$ ). Moreover, TA forest, SM forest, PA forest, PT forest, and PS forest had a relative low value of maximum water holding capacity. However, PT forest and PS forest had the second and third largest values in the semi-decomposed layer. In addition, all conifer species except AH forest ( $0.66 \pm 0.04 \text{ kg/m}^2$ ) had a higher maximum water holding capacity than broadleaved species.

**Table 4.** Litter maximum water holding rate and capacity (mean  $\pm$  SD) in different decomposition degrees. Note: Different lowercase letters indicate significant differences among tree species at the 0.05 level. U indicates un-decomposed layer and S indicates semi-decomposed layer. The abbreviation of tree species is the same as Table 1.

Forest Stands	Maximum Water Holding Rate (%)		Maximum Water Holding Capacity (kg/m <sup>2</sup> )	
	U	S	U	S
QM forest	263.27 $\pm$ 17.77 de	283.37 $\pm$ 15.12 defg	1.87 $\pm$ 0.56 a	1.74 $\pm$ 0.41 cd
BP forest	416.40 $\pm$ 32.42 b	176.29 $\pm$ 23.54 h	1.00 $\pm$ 0.18 cd	1.14 $\pm$ 0.38 def
SM forest	235.03 $\pm$ 34.12 ef	360.69 $\pm$ 19.85 bcde	0.38 $\pm$ 0.25 f	0.73 $\pm$ 0.24 ef
AS forest	331.41 $\pm$ 46.60 cd	381.32 $\pm$ 31.11 abcd	0.94 $\pm$ 0.12 cde	0.70 $\pm$ 0.13 ef
PV forest	256.40 $\pm$ 6.13 de	301.56 $\pm$ 17.23 cdefg	0.66 $\pm$ 0.13 def	0.72 $\pm$ 0.06 ef
PA forest	309.90 $\pm$ 6.68 cde	394.96 $\pm$ 13.40 abc	0.41 $\pm$ 0.11 f	0.95 $\pm$ 0.15 def
TA forest	355.89 $\pm$ 55.36 bc	440.66 $\pm$ 15.39 ab	0.25 $\pm$ 0.23 f	0.79 $\pm$ 0.11 ef
GB forest	349.02 $\pm$ 51.27 bc	281.65 $\pm$ 27.02 efg	0.73 $\pm$ 0.15 def	0.35 $\pm$ 0.21 f
AP forest	517.05 $\pm$ 44.53 a	471.01 $\pm$ 24.31 a	0.72 $\pm$ 0.35 def	1.07 $\pm$ 0.15 def
PS forest	158.90 $\pm$ 17.64 fg	257.02 $\pm$ 25.89 fgh	0.47 $\pm$ 0.11 ef	2.03 $\pm$ 0.69 c
LG forest	362.57 $\pm$ 11.61 bc	309.07 $\pm$ 19.67 cdef	0.94 $\pm$ 0.17 cde	3.82 $\pm$ 1.15 a
PT forest	158.63 $\pm$ 12.75 fg	236.50 $\pm$ 15.51 fgh	0.45 $\pm$ 0.06 ef	2.75 $\pm$ 0.21 b
AH forest	145.63 $\pm$ 14.30 g	163.38 $\pm$ 18.21 h	1.29 $\pm$ 0.18 bc	0.60 $\pm$ 0.04 ef
PK forest	135.50 $\pm$ 7.65 g	202.27 $\pm$ 22.36 gh	1.69 $\pm$ 0.06 ab	1.43 $\pm$ 0.50 cde

### 3.2.2. Litter Water Interception Characteristics

In the un-decomposed layer, as in Figure 3A, the maximum interception rate of BP forest reached 407.40%, which was 3.15 times the lowest value of PK forest, and it was significantly higher than those of other forest stands ( $p < 0.05$ ). The coniferous forest stands of PS forest, PT forest, AH forest, and PK had significantly lower values than the other stands did ( $p < 0.05$ ). Moreover, the maximum interception capacity of QM forest ( $1.81 \pm 0.74$  kg/m<sup>2</sup>) was significantly higher than those of the other stands ( $p < 0.05$ ), but there was no significant difference between QM forest and PK forest ( $p > 0.05$ ). PA forest, TA forest, and SM forest had the lowest interception capacity, which was  $0.33$  kg/m<sup>2</sup>,  $0.22$  kg/m<sup>2</sup>, and  $0.21$  kg/m<sup>2</sup>, respectively. It can be seen from Figure 2B that the maximum interception rates of TA forest, PA forest, AS forest, and AP forest were significantly higher than those of PS forest, PT forest, GB forest, PK forest, BP forest, and AH forest in the semi-decomposed layer ( $p < 0.05$ ), among which AH forest had the lowest value of 158.75%, which was just 43% of the highest value of TA forest. In addition, AH forest had the lower interception capacity in the semi-decomposed layer, but the other four coniferous species LG forest, PT forest, PS forest, and PK forest had the higher capacity (Figure 3B). In addition, the water maximum interception capacity of AS forest, SM forest, AH forest, PV forest, and GB forest were all lower than  $0.70$  kg/m<sup>2</sup>.

Figure 3C,D demonstrate the litter effective interception rate and capacity of the un-decomposed layer and semi-decomposed layer. The top three highest litter effective interception rates in the un-decomposed layer were BP forest (344.94%), AP forest (314.13%) and LG forest (300.84%), and they had significantly larger values than the other nine stands, except AS forest and TA forest, did ( $p < 0.05$ ). GB forest and QM forest had the same value with a rate of 215.09%, and the four coniferous forest stands, PS, PT, AH and PK forest, had the lowest effective interception rate. In the semi-decomposed layer, the effective interception rate of litter in each stand ranged from 134.25% (AH forest) to 328.49% (TA forest), while TA forest, PA forest, AS forest, and AP forest had significantly higher values than GB forest, PK forest, BP forest, and AH forest did ( $p < 0.05$ ). On the other hand, the effective interception capacity of un-decomposed litter was between  $0.18$  kg/m<sup>2</sup> (SM forest) and  $1.53$  kg/m<sup>2</sup> (QM forest). Except PK forest, the other forest stands had significantly lower values than QM forest did ( $p < 0.05$ ), among which the effective litter interception capacity of PT forest, PA forest, TA forest, and SM forest had the lower value, while in the semi-decomposed layer, LG forest had the highest value ( $3.73 \pm 0.44$  kg/m<sup>2</sup>), which was

16.50 times the lowest value of GB forest. The effective interception amount of PT forest, PS forest, and PK forest also had larger values. AS forest, AH forest, SM forest, PV forest, and GB forest had the lowest water interception capacity than the other species, which was only  $0.53 \pm 0.11 \text{ kg/m}^2$ ,  $0.51 \pm 0.05 \text{ kg/m}^2$ ,  $0.50 \pm 0.16 \text{ kg/m}^2$ ,  $0.50 \pm 0.05 \text{ kg/m}^2$ , and  $0.23 \pm 0.13 \text{ kg/m}^2$ , respectively.

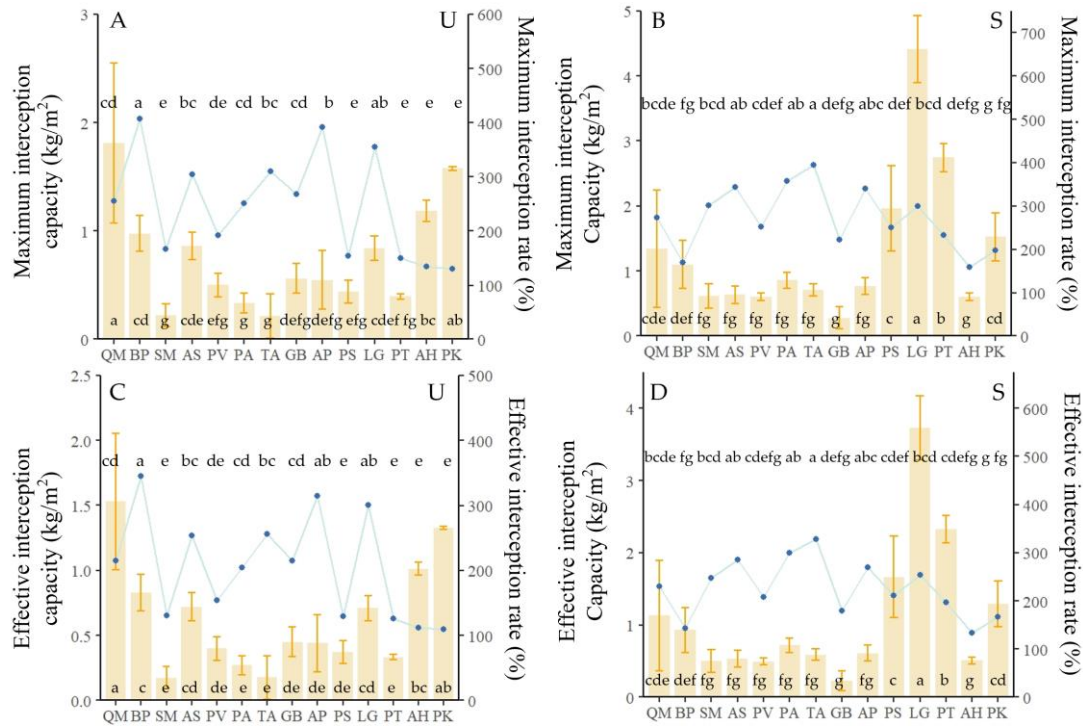


**Figure 3.** Litter water interception characteristics of different decomposed layers. (A,B) show the maximum interception capacity of 14 tree species litters in two decomposed layers, and (C,D) show the effective interception capacity of 14 tree species litters in two decomposed layers. Note: The bars are the values of maximum interception capacity or effective interception capacity, while the dots are the values of maximum interception rate or effective interception rate. Different lowercase letters within the bars indicate significant differences of water maximum interception capacity or effective interception capacity among tree species at the 0.05 level, and the lowercase letters above the dots indicate significant differences of water maximum interception rate or effective interception rate among tree species at the 0.05 level. U indicates un-decomposed layer and S indicates semi-decomposed layer. The abbreviation of tree species is the same as Table 1.

### 3.3. Summary of Litter Accumulation and Water-Related Parameters

The total litter accumulation as well as the quantity in different decomposed layers of PK forest and LG forest were significantly higher than those of other species ( $p < 0.05$ ). In the un-decomposed layer, QM forest had the strongest water holding capacity, and the values were much higher than the second place of PK forest at any time within 0–24 h. In addition, the water absorption rate and the maximum water holding capacity of QM forest were higher in this layer, while LG forest had the largest water holding capacity and water absorption rate in the semi-decomposed layer. The maximum water interception rate and effective water interception rate were highest in BP forest, with 407.40% and 344.94%, respectively, and QM forest had the significantly largest maximum water interception capacity ( $1.81 \text{ kg/m}^2$ ) and effective water interception capacity ( $1.53 \text{ kg/m}^2$ ) in the un-decomposed layer than the other forests ( $p < 0.05$ ). In addition, PK forest had a higher water maximum interception and effective interception value in both layers.

## 4. Discussion

### 4.1. The Relations between Litter Accumulation and Its Water Holding Ability

Forest litter plays an important role in hydrologic cycling [48], while the litter mass and the proportions of different decomposed layers influence the rainfall recycling process [52]. In this study, we chose to collect litters at the end of November, because in this period, the leaves of most tree species have fallen, which was the maximum accumulation of litters in the whole year, so it can reflect the maximum potential of litters to regulate precipitation. A higher litter accumulative amount indicated better ecosystem circulation, which contributes to enhancing the ecological services including water conservation [53,54].

Litter accumulation was affected by the surrounding environmental conditions, which was not only restricted by natural climate, altitude, and soil conditions, but also affected by their own growth characteristics, canopy density, and vertical structure of the stand [55]. This study revealed that the total accumulative quantity of PK and LG forest was higher, among which the un-decomposed layer of PK forest accounted for a higher proportion, which might be because the litters of PK forest contained oil and most of them had developed cuticles, so the decomposition was difficult and needed a longer time [56]. However, the accumulation in the semi-decomposed layer was higher than the un-decomposed layer in LG forest, which was probably caused by the ecosystem environment where the LG forest was located. The forest stand size of LG was large enough, so its ecological system was stable and sustainable [57]; therefore, the decomposition capacity of litters was stronger. On the other hand, there was a positive correlation between canopy density and litter accumulation. The canopy density of QM forest, PS forest, LG forest, AH forest, and PK forest was larger than that of other stands (Table 1), and the litter accumulation of the five stands was also higher (Table 3). Furthermore, due to the stable ability of substance circulation and energy exchanges of larger trees, they could produce and store a larger amount of litter [58]. For example, LG forest, PT forest, AH forest, and PK forest had a larger DBH than other types (Table 1) and corresponded to a larger litter accumulative value (Table 3). The forest density in urban parks is usually lower than that of natural forest, so the living space of urban forest was large enough for the spread of their branches and leaves. Under such circumstances, the taller the tree, the more luxuriant the branches and leaves, and the higher the utilization rate of light energy, which increased the photosynthetic capacity and the accumulation of organic matter [59]. Therefore, it helped to further elucidate the reasons for the high litter storage of coniferous species.

In addition, the litter accumulative quantity was a parameter to calculate the maximum water holding capacity, the maximum water interception capacity, and the effective water interception capacity (Table 2). Although the litter maximum water holding rate, maximum water interception rate, and effective water interception rate of QM forest in the un-decomposed layer were not too high, its capacity of maximum water holding, maximum water interception, and effective water interception were largest (Figure 3), due to its large accumulative amount (Table 3).

### 4.2. Tree Species Selection for Urban Flood Mitigation

Most of the urban flooding events were caused by the short periods of heavy rainfall [12], and the water absorption rate of litters, especially the rate within an hour, reflected the ability of urban trees to intercept rainfall for a short time. With high water absorption rate, forest litters can soak up precipitation faster, thus effectively slowing down the formation of surface runoff. It was concluded that QM forest and BP forest had the largest water absorption rate in the un-decomposed layer (Figure 2I,J). In particular, the water absorption rate of QM forest in 5 min was more than twice the second place of BP forest, and after 1 h of immersion in water, the absorption rate was even larger than the 5 min rate of PT forest, PA forest, and AH forest. On the other hand, PT forest, LG forest, and PS forest had a lower water absorption rate. This may be caused by the shape and nature of the leaf. It was reported that the larger the relative surface area of litter, the greater the water holding capacity [60]. QM leaves have a larger surface area and more network branches on the sur-

face, so they have more precipitation storage space and more water holding capacity. As for PT forest, LG forest, and PS forest, their litters contained non-hydrophilic oils and cuticles, which was not compatible with water, thus reducing their water absorption capacity [56]. Nevertheless, the coniferous species had a larger water absorption rate compared to most other broadleaved species (Figure 2K,L) in the semi-composed layer. Specifically, LG forest, PK forest, and PT forest ranked top three in highest water absorption rate. This was because after the decomposition of litters, the oil content decreased and the water absorption rate increased [56]. On the other hand, in the semi-decomposed layer, BP forest demonstrated a strong ability to absorb water as well as in the un-decomposed layer (Table 4). That is to say, other than the coniferous species of LG, PK, and QM forest, BP forest could be another choice for urban flood prevention.

In addition to short-term heavy rainfall, medium-intensity but long-duration rainfall can also cause urban floods [9]. When it rains long enough, the canopy and trunk of the trees reach saturation. In this case, the water holding and interception ability as well as the accumulation of litters under the forest directly affect whether an urban flood occurs and the degree of occurrence. The maximum interception amount of litter indicates the maximum possible rainfall interception quantity of litters, while the effective interception ability indicates the actual holding capacity of litters to rainfall [56], which is related to stand type, tree density, and the decomposition degree of litters [34,37]. Our results concluded that QM forest and PK forest performed well on maximum water holding capacity, maximum water interception capacity, and effective water interception capacity of the un-decomposed layer (Figure 3). In addition, the values of these water parameters were also ranked top five in the semi-decomposed layer, which may be due to their high litter accumulative amount (Table 3). Therefore, QM forest and PK forest may be selected as ideal species for urban flood mitigation of the long-time medium-rainfall scenario. In addition, in the semi-decomposed layer, LG forest and PT forest had the largest value in maximum water holding capacity, maximum water interception capacity, and effective water interception capacity. Furthermore, the water holding and interception capacity of LG forest in the un-decomposed layer were relatively high, but PT forest had a lower water holding and interception ability, which indicated that LG forest could also be a better choice for urban parks to mitigate urban floods than PT forest.

## 5. Conclusions

Urban flood disasters bring tremendous damage to cities, have great impacts on social economy, and even directly endanger people's life and safety. For cities undergoing rapid urbanization, it is not feasible to change the underlying surface properties or characteristics and underground drainage facilities on a large scale. Therefore, in addition to the construction of artificial drainage facilities, the ecological utility of natural resources needs to be advocated for urban land resilience and sustainability. This study compared the forest litter accumulation and the hydrological characteristics of 14 common tree species in winter city parks. Some tree species could be selected as the excellent choice for mitigating urban floods in Changchun city. The results of this study might be suitable for other cities under rapid urbanization and with similar climate conditions. However, when this method is applied to other cities, the urban environment should be considered accordingly, for their unique natural and manmade conditions. By using their characteristics of high litter accumulation, and high water holding and interception capacity, forest litters in different cities could maximize their function of absorbing and permeating surface precipitation, help to solve the urban floods issue, and reduce the losses caused by water-related disasters.

**Author Contributions:** Methodology, C.Z. and Z.Z.; software, G.B. and D.Z.; validation, J.C. and M.D.; investigation, J.C., R.G. and N.F.; writing—original draft, C.Z. and G.B.; writing—review and editing, C.Z. and T.L. All authors have read and agreed to the published version of the manuscript.

**Funding:** This research was funded by the Natural Science Foundation of Jilin Province (20220101315JC; YDZJ202201ZYTS446), “The 13th Five-year Plan” Science and Technology Project of the Education Department of Jilin Province (JJKH20200560KJ), the Capital Construction Fund Project in Budget of Jilin Provincial Development and Reform Commission (2021C044-9), the Innovation Base Project of Jilin Provincial Science and Technology Department (YDZJ202102CXJD046), and the “Climbing” Program of Changchun University (ZKP202015).

**Conflicts of Interest:** The authors declare no conflict of interest.

## References

1. IPCC. *Climate Change 2022: Impacts, Adaptation and Vulnerability*; Contribution of Working Group II to the Sixth Assessment Report of the Intergovernmental Panel on Climate Change; IPCC: Cambridge, UK; New York, NY, USA, 2022.
2. WMO. *State of the Global Climate 2021*; World Meteorological Organization: Geneva, Switzerland, 2022.
3. Ministry of Water Resources of the People’s Republic of China. *China Annual Hydrological Report 2021*; Ministry of Water Resources of the People’s Republic of China: Beijing, China, 2022.
4. State Council Investigation Team of China. *Investigation Report of “July 20” Heavy Rain Disaster in Zhengzhou, Henan Province*; Ministry of Emergency Management of the People’s Republic of China: Beijing, China, 2022.
5. Ministry of Emergency Management of the People’s Republic of China. *Basic Information on Natural Disasters in China 2021*; Ministry of Emergency Management of the People’s Republic of China: Beijing, China, 2022.
6. UN Department of Economic and Social Affairs. Available online: <https://sdgs.un.org/goals> (accessed on 10 November 2022).
7. Zhou, M.; Feng, X.; Liu, K.; Zhang, C.; Xie, L.; Wu, X. An Alternative Risk Assessment Model of Urban Waterlogging: A Case Study of Ningbo City. *Sustainability* **2021**, *13*, 826. [[CrossRef](#)]
8. Zhang, Q.; Wu, Z.; Tarolli, P. Investigating the Role of Green Infrastructure on Urban Water Logging: Evidence from Metropolitan Coastal Cities. *Remote Sens.* **2021**, *13*, 2341. [[CrossRef](#)]
9. Yu, H.; Zhao, Y.; Fu, Y.; Li, L. Spatiotemporal Variance Assessment of Urban Rainstorm Waterlogging Affected by Impervious Surface Expansion: A Case Study of Guangzhou, China. *Sustainability* **2018**, *10*, 3761. [[CrossRef](#)]
10. Yin, Z.; Yin, J.; Xu, S.; Wen, J. Community-based scenario modelling and disaster risk assessment of urban rainstorm waterlogging. *J. Geogr. Sci.* **2011**, *21*, 274–284. [[CrossRef](#)]
11. Lin, T.; Liu, X.; Song, J.; Zhang, G.; Jia, Y.; Tu, Z.; Zheng, Z.; Liu, C. Urban waterlogging risk assessment based on internet open data: A case study in China. *Habitat Int.* **2018**, *71*, 88–96. [[CrossRef](#)]
12. Islam, M.R.; Raja, D.R. Waterlogging Risk Assessment: An Undervalued Disaster Risk in Coastal Urban Community of Chattogram, Bangladesh. *Earth* **2021**, *2*, 151–173. [[CrossRef](#)]
13. Chen, W.; Dong, J.; Yan, C.; Dong, H.; Liu, P. What Causes Waterlogging?—Explore the Urban Waterlogging Control Scheme through System Dynamics Simulation. *Sustainability* **2021**, *13*, 8546. [[CrossRef](#)]
14. Shahid, M.; Cong, Z.; Zhang, D. Understanding the impacts of climate change and human activities on streamflow: A case study of the Soan River basin, Pakistan. *Theor. Appl. Clim.* **2017**, *134*, 205–219. [[CrossRef](#)]
15. Cong, Z.; Shahid, M.; Zhang, D.; Lei, H.; Yang, D. Attribution of runoff change in the alpine basin: A case study of the Heihe Upstream Basin, China. *Hydrol. Sci. J.* **2017**, *62*, 1013–1028. [[CrossRef](#)]
16. Wu, J.; Sha, W.; Zhang, P.; Wang, Z. The spatial non-stationary effect of urban landscape pattern on urban waterlogging: A case study of Shenzhen City. *Sci. Rep.* **2020**, *10*, 7369. [[CrossRef](#)] [[PubMed](#)]
17. Liu, F.; Liu, X.; Xu, T.; Yang, G.; Zhao, Y. Driving Factors and Risk Assessment of Rainstorm Waterlogging in Urban Agglomeration Areas: A Case Study of the Guangdong-Hong Kong-Macao Greater Bay Area, China. *Water* **2021**, *13*, 770. [[CrossRef](#)]
18. Tehrany, M.S.; Jones, S.; Shabani, F. Identifying the essential flood conditioning factors for flood prone area mapping using machine learning techniques. *Catena* **2019**, *175*, 174–192. [[CrossRef](#)]
19. Zhang, H.; Cheng, J.; Wu, Z.; Li, C.; Qin, J.; Liu, T. Effects of Impervious Surface on the Spatial Distribution of Urban Waterlogging Risk Spots at Multiple Scales in Guangzhou, South China. *Sustainability* **2018**, *10*, 1589. [[CrossRef](#)]
20. Liu, W.; Chen, W.; Peng, C. Assessing the effectiveness of green infrastructures on urban flooding reduction: A community scale study. *Ecol. Model.* **2014**, *291*, 6–14. [[CrossRef](#)]
21. Spletozer, A.G.; Silveira, L.J.; Barbosa, R.A.; Barbosa, S.G.; Dias, H.C.T. Effect of litter on the surface runoff of a forest fragment in the Atlantic Forest. *Braz. J. Agric. Sci.* **2021**, *16*, 1–7. [[CrossRef](#)]
22. Chen, J.; Liu, Y.; Gitau, M.W.; Engel, B.A.; Flanagan, D.C.; Harbor, J.M. Evaluation of the effectiveness of green infrastructure on hydrology and water quality in a combined sewer overflow community. *Sci. Total Environ.* **2019**, *665*, 69–79. [[CrossRef](#)] [[PubMed](#)]
23. Zhang, Q.; Wu, Z.; Guo, G.; Zhang, H.; Tarolli, P. Explicit the urban waterlogging spatial variation and its driving factors: The stepwise cluster analysis model and hierarchical partitioning analysis approach. *Sci. Total Environ.* **2020**, *763*, 143041. [[CrossRef](#)] [[PubMed](#)]
24. Fletcher, T.D.; Shuster, W.; Hunt, W.F.; Ashley, R.; Butler, D.; Arthur, S.; Trowsdale, S.; Barraud, S.; Semadeni-Davies, A.; Bertrand-Krajewski, J.-L.; et al. SUDS, LID, BMPs, WSUD and more—The evolution and application of terminology surrounding urban drainage. *Urban Water J.* **2014**, *12*, 525–542. [[CrossRef](#)]

25. Chui, T.F.M.; Liu, X.; Zhan, W. Assessing cost-effectiveness of specific LID practice designs in response to large storm events. *J. Hydrol.* **2016**, *533*, 353–364. [[CrossRef](#)]
26. Mao, X.; Jia, H.; Yu, S.L. Assessing the ecological benefits of aggregate LID-BMPs through modelling. *Ecol. Model.* **2017**, *353*, 139–149. [[CrossRef](#)]
27. Pour, S.H.; Wahab, A.K.A.; Shahid, S.; Asaduzzaman, M.; Dewan, A. Low impact development techniques to mitigate the impacts of climate-change-induced urban floods: Current trends, issues and challenges. *Sustain. Cities Soc.* **2020**, *62*, 102373. [[CrossRef](#)]
28. Lancia, M.; Zheng, C.; He, X.; Lerner, D.N.; Andrews, C.; Tian, Y. Hydrogeological constraints and opportunities for “Sponge City” development: Shenzhen, southern China. *J. Hydrol. Reg. Stud.* **2020**, *28*, 100679. [[CrossRef](#)]
29. Liu, J.; Gong, X.; Li, L.; Chen, F.; Zhang, J. Innovative design and construction of the sponge city facilities in the Chaotou Park, Talent Island, Jiangmen, China. *Sustain. Cities Soc.* **2021**, *70*, 102906. [[CrossRef](#)]
30. Xia, J.; Zhang, Y.; Xiong, L.; He, S.; Wang, L.; Yu, Z. Opportunities and challenges of the Sponge City construction related to urban water issues in China. *Sci. China Earth Sci.* **2017**, *60*, 652–658. [[CrossRef](#)]
31. Armson, D.; Stringer, P.; Ennos, A.R. The effect of street trees and amenity grass on urban surface water runoff in Manchester, UK. *Urban For. Urban Green.* **2013**, *12*, 282–286. [[CrossRef](#)]
32. Li, X.; Xiao, Q.; Niu, J.; Dymond, S.; van Doorn, N.S.; Yu, X.; Xie, B.; Lv, X.; Zhang, K.; Li, J. Process-based rainfall interception by small trees in Northern China: The effect of rainfall traits and crown structure characteristics. *Agric. For. Meteorol.* **2016**, *218–219*, 65–73. [[CrossRef](#)]
33. Yang, L.; Zhang, L.; Li, Y.; Wu, S. Water-related ecosystem services provided by urban green space: A case study in Yixing City (China). *Landsc. Urban Plan.* **2015**, *136*, 40–51. [[CrossRef](#)]
34. Li, X.; Xiao, Q.; Niu, J.; Dymond, S.; McPherson, E.G.; van Doorn, N.; Yu, X.; Xie, B.; Zhang, K.; Li, J. Rainfall interception by tree crown and leaf litter: An interactive process. *Hydrol. Process.* **2017**, *31*, 3533–3542. [[CrossRef](#)]
35. Zhang, B.; Li, W.; Xie, G.; Xiao, Y. Water conservation of forest ecosystem in Beijing and its value. *Ecol. Econ.* **2010**, *69*, 1416–1426.
36. Jiang, M.-H.; Lin, T.-C.; Shaner, P.-J.L.; Lyu, M.-K.; Xu, C.; Xie, J.-S.; Lin, C.-F.; Yang, Z.-J.; Yang, Y.-S. Understory interception contributed to the convergence of surface runoff between a Chinese fir plantation and a secondary broadleaf forest. *J. Hydrol.* **2019**, *574*, 862–871. [[CrossRef](#)]
37. Li, X.; Niu, J.; Xie, B. The Effect of Leaf Litter Cover on Surface Runoff and Soil erosion in Northern China. *PLoS ONE* **2014**, *9*, e107789. [[CrossRef](#)]
38. Szota, C.; Coutts, A.M.; Thom, J.K.; Virahsawmy, H.K.; Fletcher, T.D.; Livesley, S.J. Street tree stormwater control measures can reduce runoff but may not benefit established trees. *Landsc. Urban Plan.* **2019**, *182*, 144–155. [[CrossRef](#)]
39. Richards, P.J.; Farrell, C.; Tom, M.; Williams, N.S.G.; Fletcher, T.D. Vegetable raingardens can produce food and reduce stormwater runoff. *Urban For. Urban Green.* **2015**, *14*, 646–654. [[CrossRef](#)]
40. Wu, W.; Li, L.; Li, C. Seasonal variation in the effects of urban environmental factors on land surface temperature in a winter city. *J. Clean. Prod.* **2021**, *299*, 126897. [[CrossRef](#)]
41. Hidalgo, A.K. Mental health in winter cities: The effect of vegetation on streets. *Urban For. Urban Green.* **2021**, *63*, 127226. [[CrossRef](#)]
42. Statistic Bureau of Jilin. *Jilin Statistical Yearbook*; Statistic Bureau of Jilin: Changchun, China, 2021.
43. Changchun Bureau of Statistics. *Changchun Statistical Yearbook*; Changchun Bureau of Statistics: Changchun, China, 2021.
44. Statistic Bureau of Jilin. *Jilin Statistical Yearbook*; Statistic Bureau of Jilin: Changchun, China, 2020.
45. Statistic Bureau of Jilin. *Jilin Statistical Yearbook*; Statistic Bureau of Jilin: Changchun, China, 2019.
46. Statistic Bureau of Jilin. *Jilin Statistical Yearbook*; Statistic Bureau of Jilin: Changchun, China, 2018.
47. Statistic Bureau of Jilin. *Jilin Statistical Yearbook*; Statistic Bureau of Jilin: Changchun, China, 2017.
48. Cui, Y.; Pan, C.; Zhang, G.; Sun, Z.; Wang, F. Effects of litter mass on throughfall partitioning in a *Pinus tabulaeformis* plantation on the Loess Plateau, China. *Agric. For. Meteorol.* **2022**, *318*, 108908. [[CrossRef](#)]
49. Bai, Y.; Zhou, Y.; Du, J.; Zhang, X.; Di, N. Effects of a broadleaf-oriented transformation of coniferous plantations on the hydrological characteristics of litter layers in subtropical China. *Glob. Ecol. Conserv.* **2020**, *25*, e01400. [[CrossRef](#)]
50. Wickham, H. *ggplot2: Elegant Graphics for Data Analysis*; Springer: New York, NY, USA, 2016.
51. Mendiburu, F.D. *Agricolae: Statistical Procedures for Agricultural Research*. Available online: <https://CRAN.R-project.org/package=agricolae> (accessed on 10 November 2022).
52. Neris, J.; Tejedor, M.; Rodríguez, M.; Fuentes, J.; Jiménez, C. Effect of forest floor characteristics on water repellency, infiltration, runoff and soil loss in Andisols of Tenerife (Canary Islands, Spain). *Catena* **2013**, *108*, 50–57. [[CrossRef](#)]
53. Zhao, L.; Hou, R.; Fang, Q. Differences in interception storage capacities of undecomposed broad-leaf and needle-leaf litter under simulated rainfall conditions. *For. Ecol. Manag.* **2019**, *446*, 135–142. [[CrossRef](#)]
54. Wang, B.; Niu, J.; Berndtsson, R.; Zhang, L.; Chen, X.; Li, X.; Zhu, Z. Efficient organic mulch thickness for soil and water conservation in urban areas. *Sci. Rep.* **2021**, *11*, 6259. [[CrossRef](#)]
55. Zhang, Y.; Gan, Z.; Li, R.; Wang, R.; Li, N.; Zhao, M.; Du, L.; Guo, S.; Jiang, J.; Wang, Z. Litter production rates and soil moisture influences interannual variability in litter respiration in the semi-arid Loess Plateau, China. *J. Arid Environ.* **2016**, *125*, 43–51. [[CrossRef](#)]
56. Liu, X.E.; Su, S.P. Hydrological functions of litters under five typical plantations in southern and northern mountains of Lanzhou City, Northwest China. *Chin. J. Appl. Ecol.* **2020**, *31*, 2574–2582.

57. Yang, Y.; Bao, G.; Zhang, D.; Zhai, C. Spatial Distribution and Driving Factors of Old and Notable Trees in a Fast-Developing City, Northeast China. *Sustainability* **2022**, *14*, 7937. [[CrossRef](#)]
58. Ali, A.; Wang, L.-Q. Big-sized trees and forest functioning: Current knowledge and future perspectives. *Ecol. Indic.* **2021**, *127*, 107760. [[CrossRef](#)]
59. Bordin, K.M.; Esquivel-Muelbert, A.; Bergamin, R.S.; Klipel, J.; Picolotto, R.C.; Frangipani, M.A.; Zanini, K.J.; Cianciaruso, M.V.; Jarenkow, J.A.; Jurinitz, C.F.; et al. Climate and large-sized trees, but not diversity, drive above-ground biomass in subtropical forests. *For. Ecol. Manag.* **2021**, *490*, 119126. [[CrossRef](#)]
60. Zhao, W.; Li, K.; Wang, J.; He, Z. Litter water-holding capacity and accumulation amount of five Acacia plantation. *J. Sichuan Agric. Univ.* **2020**, *38*, 677–684.